Understanding the effect of Spin-state on the Seebeck Coefficient of Iron Doped Barium Titanate (Fe-BTO) via Molecular Beam Epitaxy for high-efficiency thermoelectric applications

A Dissertation Proposal Presented

By

Sue-Jonnathane Celestin

to

The Department of Chemical Engineering

In partial fulfillment of the requirements

For the degree of

Doctor of Philosophy

In the field of

Chemical Engineering

Northeastern University

Boston, Massachusetts

(December 12th, 2016)

ABSTRACT

A longstanding objective of the broader materials research community is the development of high-efficient thermoelectric (TE) materials for devices that can recover electrical energy from warm sources. Despite the new approaches that saw an increased interest in thermoelectric energy conversion, the challenge of achieving improved efficiency in TE materials still remains. Literature shows that obtaining separate control over the electronic and thermal properties of materials is necessary for high performance TE materials.

A promising material for TE application is iron doped barium titanate (Fe-BTO). It is hypothesized that under the correct atomic arrangement, the spin state of the iron atom can be changed such that the material has a strong Seebeck coefficient without influencing negatively the thermal conductivity or the electrical conductivity of the material. Molecular beam epitaxy (MBE), a method which provides control of crystal growth at the atomic level will be used to grow Fe-BTO thin films on 6H-SiC. A series of experiments is proposed to study and to understand the influences of thin film growth processing parameters on thin film spin state. Structure and chemistry will be related to processing conditions and then to the resulting spin state. The correlation of processing conditions to film characteristics and thermoelectric properties, will allow hypothesis about growth mechanisms to be developed in order to engineer growth processes for thin films with desired characteristics and thermoelectric properties.

TABLE OF CONTENTS

LIST OF FIGURES

1.0 Introduction

While the search for better fuels continues, investments in energy efficiency have the potential to provide savings capable of decreasing our annual energy needs. One opportunity to improve overall energy efficiency is to recover energy lost as heat from other mechanical or electrical processes such as heat lost from engines, using thermoelectric (TE) materials

However, in order to truly enable high energy efficient systems for waste heat recovery, TE materials must be more efficient then what is available today. TE efficiency is defined as ZT, the accepted Figure of Merit that quantifies performance of a TE material. Current standards include materials and related alloys of lead, tellurium and germanium with ZT of approximately 1 which implies that TE devices with such materials can operate at a power conversion efficiency of 4%–5% [1]. However a ZT of 3 or greater is needed for next generation TE materials in order to address many of the energy-related challenges.

Recently predictions have been made about alternative TE material engineering approaches using low dimensional structures that can enable the ZT value to be pushed to 1.9 by reducing the thermal conductivity [2] However, the high-temperature stability, cost effectiveness, and toxicity of these materials is an issue for applications such as powering sensors for electrocardiograms and high-temperature heat harvesting. Oxides of less toxic materials such as barium titanate ($BaTiO_3$, and ZnO) provide promising alternatives due to their high- temperature stability and high tunability. However, the conversion efficiency of these oxides as currently grown are generally low (ZT~0.3) [1] [30]. Material properties such as thermal conductivity, electrical conductivity and Seebeck coefficient have a direct influence on ZT (full equation development follows in Chapter 2). While each property affecting the ZT can be increased independently by several orders of magnitude, their interdependence and coupling limits the overall ZT. Therefore, research efforts focused on creating advanced materials where each desired property can be manipulated independently to effectively maximize ZT.

The proposed research will take advantage of metal oxide's tunable electronic and phonon transport to understand the role of spin state imbalance in enhancing the Seebeck

coefficient in metal oxide. This work will use molecular beam epitaxy (MBE) as a growth technique to control atomic level stoichiometry and structure so that the relationships between processing conditions, structure/chemistry, spin state and TE transport properties can be understood. In order to achieve this goal, the following three objectives will be met.

1) Establishing operation conditions for single crystalline, stoichiometric epitaxial growth of BTO (111) on 6H-SiC and understand the variations in growth conditions in order to identify potential influences on the spin state of the metal in the oxide.

2) Using the information learned in Objective 1 to understand the effects of processing parameters on the incorporation of Fe in single crystalline BTO, in order to help understand the influences of the MBE processing parameters on iron doping

3) Using the information learned in Objectives 1 and 2 to correlate processing conditions to film characteristics to metal spin state in order to form a solid relationship between spin state and Seebeck coefficient

2.0 Background

2.1 Introduction to thermoelectric materials

This section presents an overview of the theory behind TE materials and historical approaches to maximizing the figure of merit, ZT, in order to elucidate recent advances that will be discussed in chapter 3: Literature review. This will set the theoretical foundation for the proposed research.

2.1.1 Fundamental principle behind thermoelectricity

Thermoelectricity is the direct conversion between heat and electricity. The observed phenomenon is called the thermoelectric effect. The term "thermoelectric effect" encompasses three separately identified effects: The Seebeck effect, the Peltier effect, and the Thomson effect. The Seebeck effect is the conversion of temperature differences directly into electricity [3]. Figure 1 illustrates two of the phenomena. All materials exhibit thermoelectric effects but to be commercially viable, materials need to have a Figure of Merit (described later) of 1 or greater.

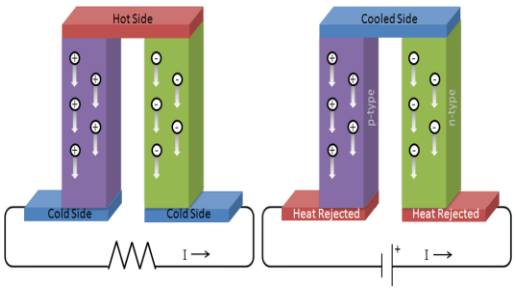

Figure 1: Schematic of a p-n junction used as a thermoelectric couple based on two major thermoelectric effects: Peltier effect on the right and Seebeck effect on the left. [4]

When two dissimilar conducting materials are connected in a junction to form a thermocouple, the application of a temperature at the junction, that is different from the electrically isolated ends of the individual wires, will produce a voltage across the unpaired terminals. This voltage is called *the relative Seebeck electromotive force*, RSE and the instantaneous rate of change of the absolute Seebeck emf is the absolute Seebeck coefficient [5].The performance of any thermocouple as an energy convertor depends on the thermal and electrical properties of the two materials forming the junction. However in the search improved thermocouples, it is uncommon to investigate a pair of materials at the same time. Therefore single material properties will be the focused in the following discussions.

When electrons in a material are subjected to a temperature difference they flow from the hot end to the cold end causing an electric current. Therefore a high flow of electrons is necessary to maximize the electrical current going through a material and a low flow of heat carrying particles is necessary to maintain a large temperature gradient. The key parameters that are used to describe the magnitude of the Seebeck voltage are the Seebeck coefficient, the electrical conductivity and the thermal conductivity. The Seebeck coefficient, S, of a material is defined by the following equation

$$S = \frac{8\pi^2 k_B^2}{3eh^2} m^* T \left(\frac{\pi}{3n}\right)^{2/3} \quad (1)$$

Where k_B = Boltzmann constant

n = carrier concentration

m* i= effective mass of the charge carrier

h = plank's constant

A high Seebeck coefficient, S, is required to get the maximum output voltage per degree of temperature difference. Electrical conductivity is the ability of a material to conduct an electrical current. This value needs to be at its maximum in a thermoelectric material to minimize the loss of charge energy due to joule's heating which is the process where the energy of an electric current is converted to heat as it flows through the material [27].

In the Drude model, the electrical conductivity given in equation (2) is defined in terms of the elastic scattering time, τ, and the effective mass of the electrons,m^*.

$$\sigma = \frac{nq^2\tau}{m^*} \quad (2)$$

Where:

n is the carrier density

q is the charge of the electron

When the material is subjected to a temperature difference, a fraction of heat will be directly transported from the hot side of the couple (T_h) to the cold side of the couple (T_c) through thermal conduction rather than being carried by charges. The part of the heat carried directly from one side to the other will not produce electricity hindering the achievement of high conversion efficiency while maintaining a high temperature difference.

Heat is carried in solid materials by lattice vibration waves (phonons), and by free electrons. Therefore, the ability for a solid to conduct heat, the thermal conductivity, is the summation of the lattice contribution k_{ph} and the electron contribution k_e. A low thermal conductivity, κ, is highly favored to enable restriction of the diffusion of the heat across the device in order to maintain a large temperature gradient. The Seebeck coefficient, the electrical conductivity and the thermal conductivity of a given material are embodied in the so-called figure-of-merit, Z. Since Z varies with temperature, a useful dimensionless figure-of-merit can be defined as ZT. The Figure of Merit of a single material is given by:

$$Z_iT = \frac{\sigma S^2 T}{\kappa_{lattice}+\kappa_{electronic}} \quad (3)$$

Where:

S is the Seebeck coefficient of the material

σ is the electrical conductivity

$\kappa_{lattice}$ or κ_{ph} = phonon contribution to the thermal conductivity

$\kappa_{electronic}$ or κ_e = electronic contribution to the thermal conductivity.

T is the absolute temperature

Based on the relationship describe in equation (3), obtaining a high Figure of Merit for thermoelectric materials requires maintaining high electrical conductivity and large Seebeck coefficient while simultaneously limiting thermal conductivity.

In a simple material, an increase in Seebeck coefficient, S, leads to a simultaneous decrease in electrical conductivity, σ. Comparatively, an increase in electrical conductivity σ, leads to an increase in thermal conductivity, κ_e. The dependence of the parameters as a function of carrier concentration is illustrated in Figure 2

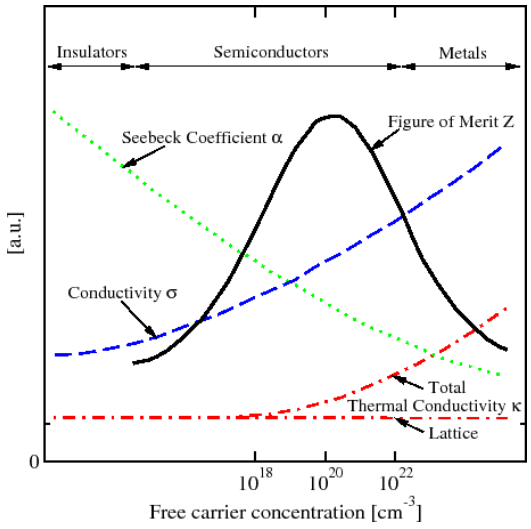

Figure 2: Illustration of the interdependence of the Seebeck coefficient, the Figure of Merit, the electrical conductivity and the thermal conductivity with respect to the change in carrier concentration for a bulk material. [5]

While increasing the carrier concentration is unfavorable to the Seebeck coefficient, Figure 2 shows an increase in electrical conductivity due to the increase of available carriers. On the other hand as the carrier concentration increases in metals the electronic contribution to the thermal conductivity becomes dominant [6]. Metals are

usually known for their low values of Seebeck coefficient (10 μV/K), high thermal conductivity and high electric conductivity, which cannot compensate for the former two setbacks. The insulators are characterized by high Seebeck coefficient (~2000 μV/K) and low electrical conductivity. Semi-conductors seem to have a carrier concentration in the range where the Figure of Merit is at its maximum while parameters compete with each other, making semiconductors with low lattice thermal conductivity, κ_{ph} and high Seebeck coefficient one of the target thermoelectric materials.

2.2 Historical work on Semiconductor Thermoelectric materials

Two predominant approaches have been adopted to improve the material's Figure of Merit. The first approach is called the "Phonon glass electron crystal" (PGEC) and the second approach is nanostructuring. The former approach led to the engineering of complex materials with distinct region aimed at providing different functions[7].The second approach involves the decrease in size of the material from bulk to the nanometer scale forming what is called low dimensional materials possessing at least one physical boundary small enough to confine the electrons or phonons [7].

Low dimensional thermoelectric materials were introduced as a mean to improve the ZT by modifying the trade-off between bulk properties. The unique ability to tune material properties by reducing the size to low dimensional structures brought the introduction of nanoscale polycrystalline and interfaces into bulk materials which have the potential to reduce the lattice thermal conductivity by increasing the phonon scattering without compromising carrier mobility values. This is possible at the nanoscale because when the dimension of a material is made smaller than the mean free paths of electrons and low frequency phonons, the boundary of the material confines the mean free paths to those of high and medium frequency phonons. This essentially screens out the low frequency phonons and decreasing the thermal conductivity without touching the electrical conductivity. For Seebeck coefficient, low-dimensional systems at a given carrier concentration is expected to be enhanced over that of bulk materials because of size-quantization effects.

2.3 Thermoelectric oxides

The reliance on current TE materials such as PbTe is troublesome partly because of their toxicity (Sb, Se, Pb), which will limit material applications, but more so because of the scarcity and cost of tellurium which at 1 ppb in the earth‘s crust is even rarer than platinum (37 ppb). Because of its scarcity the cost of tellurium has risen from $3.86/ lb in 2000 to $127/ lb as of 2015 [9]. In comparison, oxide thermoelectrics are generally non-toxic and rely on more abundant transition metals, having excellent high temperature stability and corrosion resistance. Metal oxides are also known to exhibit a wide range of electronic properties ranging from insulating to semiconducting to conducting which make them quite promising in terms of tuning their electrical property [8]. However this class of compound was initially overlooked in the search for high ZT materials because, typically insulators, they exhibit very low electrical conductivity and most also have a low average atomic mass relative to many traditional thermoelectric materials and therefore a higher atomic vibration frequency and thermal conductivity. However, a case can be made for the use of metal oxides as thermoelectric materials based on a large value of the Seebeck coefficient that can potentially be obtained, as well as the electrical tunability available in the typically complex structures.

2.3.1 Strongly correlated systems and Seebeck coefficient

In a solid, the flow of electrons is accompanied by both a charge current and an entropy current. This entropy current is also part of the Seebeck effect, and in oxide materials, the electronic spin entropy (or in other words the energy carried by moving spin) is predicted to dominate the entropy current thus, impacting spin entropy in oxide materials is believed to impact the Seebeck effect. When any material is subjected to a temperature gradient, electrons flow from the hot side to the cold side generating an electric current.

As electric current caused by charge accumulation is indifferent to spin, a magnetic field should have virtually no effect on the Seebeck coefficient. However, Wang *et al.* found a suppression of the Seebeck coefficient under a longitudinal magnetic field at low temperature (10K) in $NaCo_2O_4$ [10]. These experimental results and many other investigations disclosed that spin entropy plays some sort of role in influencing the

Seebeck coefficient. Thus, this is more evidence of the possibility of controlling spin entropy in order to influence the Seebeck coefficient.

2.3.2 Spin state of a material

An oversimplification often occurs where only the entropy from charge is considered ignoring the fact that the carriers also have spin and orbital degrees of freedom. In metals the spins are tied to delocalized electrons but in compounds like $NaCo_2O_4$ the spins are not fixed to specific atoms within the lattice, and instead they are free to move around. This class of compound in which spins are delocalized is called strongly correlated systems. Strongly correlated electron systems have degenerate 3d orbitals due to electron spin and orbital degree of freedom. This orbital degeneracy permits the material to either be in a high spin state or a low spin state. A metal with an electronic configuration that contains the maximum number of unpaired electrons is said to be high-spin. While the electronic configuration with the minimum number of unpaired electrons other is called low-spin.

Theoretically, three interacting factors affect the spin state of a material: The field effect geometry, the oxidation state of the metal center and the electron d-configuration.

1. Field geometry:

Whether a crystal is high spin or low spin depends on the relative size of the pairing energy (P), which is the energy needed to pair two electrons and the splitting energy (Δ) defined as the energy distance between bands. If $P > \Delta$, the crystal will be high spin. If $P < \Delta$, the complex will be in low spin. However, metal ions in an octahedral field are more likely to have the option to be in high-spin or a low-spin state because of its higher splitting energy (Δ_o) [11].

2. Oxidation state of metal:

It has been observed that the greater the charge on the metal ion, the greater the magnitude of the splitting energy, Δ.

3. Electron d-configuration

Octahedral bonding geometry of materials with electron configuration of d1, d2, d3, d8, d9, d10 only have one way to arrange the electrons. As a result, only when there are four, five, six, or seven electrons in the *d* orbitals, can the electrons be rearranged in ways to change from high-spin to low-spin materials [11].

Understanding how those three key interacting factors can be manipulated in metal oxides and how they influence the spin state of metal oxides can allow further correlations between spin state and Seebeck coefficient. The goal is to understand the mechanism of spin interaction in a way that opens up possibilities for spin state tuning.

2.4 Thin film Barium titanate ($BaTiO_3$, BTO)

The absence of lead and the physiological inertness of Barium titanate (BTO, $BaTiO_3$), has made it an ideal material for many applications. Due to its high temperature stability Barium titanate has the potential advantage over conventional semiconductor for thermoelectric devices operating at very high temperatures of 1000K and above. Adversely, BTO like most of the metal oxides is known to have a high thermal conductivity compared to the threshold value wanted for ideal thermoelectric materials. Therefore in order to enable BTO as a practical thermoelectric material, we need to take advantage of the influence of spin state on the Seebeck coefficient.

As discussed previously, spin-state in bulk materials can be influenced by three factors. In Thin film, the manipulation of those three factors can be most directly impacted by the following means:

1. The field effect geometry, which involves change in crystallinity, relative atom placement (substitution site), substrate, and dimensional constraints.
2. The oxidation state of the metal center or the bonding of oxygen (O) to metal
3. The d configuration, which involves the choice of a dopant metal of 4 to 7 electrons in the d orbital.

Experimentally, the transition between high-spin and low–spin state in inorganic bulk materials has been attributed to the incorporation of dopants (including iron, cobalt, and manganese which have magnetic moments) that impact the spin, or by applying pressure leading to a thermal spin switch. However, in thin films, the low dimensional geometry creates a localized effect (discussed in section 2.2) that may enable tuning of the spin with dopants or crystal defects for targeting desired transport properties. To explore the spin state contribution to Seebeck coefficient of thermoelectric oxides, Fe-doped Barium titanate (Fe-BTO) thin film will be engineered via MBE to understand and study how growth conditions can be used to tune the spin-state of oxides.

2.4.1 Barium titanate structure, $BaTiO_3$ (BTO)

The crystal structure of BTO is given in the following Figure 3.

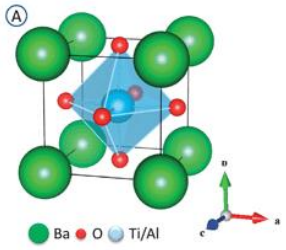

Figure 3: Crystal structure of BTO. Green atom is barium and blue-red octahedral are TiO_6 [12]

BTO adopts the perovskite (ABO_3) structure with Barium ions occupying the corner sites, titanium ions located at the centers of the cube (the oxygen octahedral) and the oxygen anions are on the face-centers. The lattice type is cubic with a = 4.009 A. The geometry around the Ti^{4+} ion is ideal for a potential competition between pairing energy (P) and crystal field energy leading to a crystal in either high-spin or low spin. However the electron configuration of Ti^{4+} and Ti^{3+} are *d0* and *d1* respectively which falls under the category of metal with only one possible electron configuration with high-spin state. Metal ions in an octahedral field with four, five six or seven electrons in the d orbitals have the ability to be in high-spin or a low-spin state. Therefore, what is needed is a metal that has the right d-electron configuration that will allow the manipulation of the spin state of BTO

A free iron atom has an electronic configuration of [Ar] 3d6 4s2. An iron ion of Fe^{2+} has an electron configuration of [Ar] 3d6, Fe^{3+} has a configuration of [Ar] 3d5 and Fe^{4+} has a configuration of [Ar] 3d4. Therefore, all three possible valence states of the metal have the potential of being in the low spin state which makes iron –doping of BTO of great interest. Controlling the oxidation state of iron in BTO will likely have significant impact on the BTO film properties. With MBE we can discover how to tune the iron oxidation state during film growth.

2.5 Epitaxy and Atomic mismatch

Epitaxy is defined as the extension of the crystal structure from a crystalline substrate [13]. There are two types of epitaxy: homoepitaxy and heteroepitaxy.

Homoepitaxy refers to epitaxial film growth where the film and substrate are the same material with the same crystal structure and orientation. Heteroepitaxy refers to film growth where the film is a different material than the substrate yet retains the atomic structure alignment with the substrate. An example of heteroepitaxy is the growth of BTO on a SiC substrate, denoted (BTO/SiC), which is the primary focus in this proposal. Heteroepitaxy is more complex because the growth must accommodate compatibility issues between the film and substrate. These issues include, but are not limited to, lattice mismatch, chemical interactions, and thermal mismatch.

Lattice mismatch is a difference in the lattice parameter of the bulk film material from the lattice parameter of the bulk substrate material. The lattice mismatch can be defined by the following equation:

$$\text{Lattice mismatch: } \frac{a_{i+1}-a_i}{a_{i+1}} \times 100 \qquad (4)$$

Where $a_{i+1}$is the bulk lattice parameter of the subsequent film and a_i is the bulk lattice parameter of the substrate.

These lattice parameters refer to the unstrained lattice parameters of the substrate or the film and are defined as the length of one unit cell of the crystalline material. During film growth, the lattice mismatch between the film and substrate need to be absorbed within the growing film. Therefore, it is not uncommon for the lattices to be strained and deviate from bulk values without defect formation. As a result, the lattice parameter of the thin film often differs from the lattice of parameter of the bulk material. When the lattice mismatch is a negative value, the film is under tensile strain. When the lattice mismatch is positive, the film is under compressive strain [14]. These strains can propagate causing various defects in the films. If the lattice mismatch between the film and substrate is too large, the resulting film is often polycrystalline or even amorphous.

In addition, using an interlayer or template layer between the substrate and the thin film can improve the quality of the resulting film both by one of three strategies: 1) eliminating reactions between the semiconductor substrate, 2) providing a more favorable lattice match on which the film can nucleate, or 3) enabling chemical mechanisms to align the film [15]. Templates are thin films of a few nanometers thick, which are designed to enable one of the strategies in order to serve as a bridge between the substrate

and film. The lattice parameter of a template material often lies between that of substrate and film.

The use of a template layer may enable the growth of single crystal films; however, its use changes the interfacial properties. As a result, the performance of the ultimate device may be limited by or enhanced an interlayer, depending upon the desired end-use of the hetero-structure. Consequently, there may be a trade-off between effective integration of tetragonal metal oxides with the wide bandgap semiconductor (requiring a template layer) and film properties.

2.6 Thin film characterization

The characterization techniques involved in this study consist of *in-situ* (sample is not exposed to laboratory air) and *ex-situ* (outside of the vacuum chamber) techniques. *In-situ* reflection high energy electron diffraction (RHEED) is used to monitor the crystallinity and measure the surface atomic arrangement for single crystal surfaces and surface reconstruction. X-ray photoelectron spectroscopy (XPS) is used to measure atomic stoichiometry of the films and bonding states of the atoms. Atomic force microscopy (AFM) is used to measure surface morphology and Transmission electron microscopy (TEM) is use to image atomic structure. In addition to film characteristics the thermoelectric properties and spin properties are measured by a DC- 4 probe method and superconductive quantum interface device (SQUID) respectively.

3.0 Critical literature Review

The current research into the Seebeck coefficient of TE oxide materials focuses mostly on understanding Seebeck enhancement in bulk oxides materials. In order to understand the source of Seebeck coefficient enhancement, spin interactions need to be understood at the atomic scale. A more detailed look at relevant studies of doping concentration, oxygen vacancies, strain, and unit cell volume on spin in bulk and thin film metal oxides can incorporate findings and understanding necessary to enable the tuning of the Seebeck coefficient for thermoelectric applications.

3.1 Influence of dopant concentration on spin state and Seebeck coefficient

Experimentally, high- spin metal ions in transition metal oxides demonstrate a suppression of the Seebeck coefficient while low-spin metal ions enhance the Seebeck coefficient. This has been observed in Terasaki *et al.* [17]. They found that $NaCo_2O_4$ bulk crystals exhibited metallic electrical conductivity (0.2 mΩ cm), and a large Seebeck coefficient of 100 μV/K at room temperature with an increase in the Seebeck coefficient (200 μV/K) at high temperatures. The bulk crystal Na ions and CoO_2 are alternately stacked along the c-axis and the cobalt ions exist in a mixture of Co^{3+} and Co^{4+}. The magnetic measurements of both Co ions revealed that they are in a low spin state and the spin state may be the source of the enhanced Seebeck coefficient [16]. The low spin state of cobalt ions enables the hopping of an electron from one oxidation state to another resulting in a large entropy exchange between Co^{3+} and Co^{4+}. This entropy exchange was added to the original Heikes formula and a new modified version of the Heikes Formula was derived and is given in equation (5)

$$S = \frac{k_B}{q} \ln\left(\frac{g_I}{g_{II}} \frac{\gamma}{1-\gamma}\right) \qquad (5)$$

Where the subscripts I and II denote the conduction sites and g_I and g_{II} denote the electronic degeneracy associated with each site respectively.

Equation (5) demonstrates that not only the fraction of conducting sites [y/ (1-y)] but also the ratio of the degeneracies for the ions involved in conduction is equally important. Therefore, for a stoichiometric compound $NaCo_2O_4$ with cobalt ions $[Co^{3+}] = [Co^{4+}] = 0.5 = \gamma$ in low spin states, applying the electronic degeneracy $g_{3+}= 1$ and $g_{4+} = 6$ and substituting in equation (5) we get a Seebeck coefficient of 154 μV/K which is in good agreement with the low- temperature experimental Seebeck coefficient of 100 μV/K in bulk crystals of $NaCo_2O_4$ [17]. The large Seebeck coefficient stems from the presence of the low-spin state of Co^{3+}. Along the same line, if both Low spin and high spin states are available to Co^{4+} ions then the total contribution of Co4+ ion is the sum of the contribution of the low spin and the high spin state given by $g_{4+} = 6+6 = 12$ which when substituted in Eqn. 8 gives a calculated Seebeck coefficient of 214 μV/K. This value of the Seebeck coefficient also is in good agreement with the high-temperature transition observed in the Seebeck coefficient which suggests that having a low spin state may not

be the only route to a high Seebeck coefficient but rather, having a high degeneracy ratio is necessary to an increase in Seebeck coefficient.

Similarly, Kobayashi *et al.* [18] found that bulk $Sr_{1-x}Y_xCoO_{3-y}$ (SYCO) is also a layered structure where octahedral CoO_6 and tetrahedral/pyramidal $CoO_{4.25}$ layers are alternately stacked with insertion of the ordered $Sr_{0.75}Y_{0.25}O$ layer. The Co ions in the CoO_6 layer occupy the intermediate spin state and those of the $CoO_{4.25}$ occupy the high spin state. Ca^{2+} was used as a dopant and Seebeck coefficient was observed to be strongly dependent on Ca^{2+} content. The results showed that with increasing dopant content from x = 0 to x = 0.8 the magnetization drops from 4.5 emu/g to 1 emu/g with a decrease in the transition temperature which is associated with the spin state cross over between intermediate spin and low spin. The Seebeck coefficient was also seen to change with the Ca content: at 100 K, the Seebeck coefficient for x= 0 is 60 μV/K, whereas that for x = 1.2 is 200 μV/K. Since the resistivity is essentially the same value between x = 0 and x= 1.2 the Seebeck coefficient and the thermoelectric Figure of Merit $Z = S^2/\rho\kappa$ are enhanced by a factor of $(200/60)^2 \sim 13$. The Seebeck coefficient enhancement can be understood in terms of the spin-state cross over driven by chemical pressure, in other words pressure due to strain induced by the dopant. Since the Ca ion is divalent (2+), its substitution acted as a chemical pressure which drives the spin state of Co^{3+} from the high/intermediate spin state to the low spin state as is similar to many other oxides. [19][20]. Also one interesting effect that was observed is that the electrical resistivity seems to be almost independent of the Ca substitution. At 800 K, the resistivity is as low as 2-3 mΩ cm which corresponds to that of conventional metals. These results are promising for isolation of interdependent properties.

In order to understand how the doped transition metal Fe affects the spin entropy, Tang *et. al* [21] studied the magneto-Seebeck coefficient, Mössbauer spectra and magnetic properties in Fe- doped bulk $NaCo_2O_4$ in detail. They found that high-spin Fe^{3+} doping suppresses the spin entropy in $NaCo_2O_4$ and reveal the reason for the decrease in Seebeck coefficient. The temperature dependence of the Seebeck Coefficient for $NaCo_{2-x}Fe_xO_4$ (x = 0, 0.1, 0.4, and 0.6) was generated. The Seebeck coefficient for all samples was seen to increase monotonically with the elevated temperature. However the Seebeck coefficient decreased with the increase in Fe content across the entire temperature range [21]. In order to disclose the effect of Fe doping on spin entropy,

Mössbauer spectra and magnetic properties were also studied for these materials. For all Fe- doped samples, the molar magnetic susceptibility, χ, is enhanced by Fe doping in the studied temperature range. This can be attributed to the substituting of high-spin Fe^{3+} ions for nonmagnetic Co^{3+} ions. The effective magnetic moment, $\mu_{eff,}$ is seen to decrease with decreasing temperature for all samples, suggesting antiferromagnetic coupling in the (Co, Fe) O sublattices. The μ_{eff} for the undoped sample is 1.29 μ_B at 40 K, in good agreement with the low-spin configuration of Co^{4+} (S = 1 /2) and Co^{3+} (S = 0) ions. The μ_{eff} for all doped samples with x =0.1, 0.4, and 0.6 is enhanced across the entire studied temperature regime, suggesting that partial nonmagnetic Co^{3+} ions are replaced by high-spin Fe^{3+} ions, inducing the increase in the average quantum number of spin and then the increase in μ_{eff}.

Based on the above studies, it can be concluded that both the concentration of metal ions and the oxidation state in which it is present contributes to the spin state of the material. While, the effect of doping with transition metals on thermoelectric property of $NaCo_2O_4$ is generally studied [22] [23], studies about the effect of transition metal doping on the spin entropy are very few. In cobalt oxides, the spin entropy contribution to the Seebeck coefficient is related to the Co^{4+} concentration and degeneracy [21]. However, this relationship needs to be explored in other metal oxides. Investigating the effect of transition metals doping on the spin entropy may promise an effective way for improving the Seebeck coefficient.

3.2 Influence of Crystallographic unit cell volume on spin state of metal

In order to understand how to tune the spin state, an understanding of the spin state transition with respect to the Seebeck coefficient is necessary. Experimentally, the transition between high-spin and low- spin state has been attributed to applying pressure, increasing the temperature leading to a spin switch [24] [25]. Many studies relate the transition from high spin to low spin to an applied pressure inducing a shift from high spin to low spin states, which is a direct consequence of the lower volume for the low spin molecule. Studies by Kobayashi *et al.* [18] and by Tang *et al*. [21] attribute the spin state transition of the metal ion to a change in unit cell volume. When the spin state of the metal ion goes from high/intermediate spin to low spin, it is accompanied by a decrease

in unit cell volume whereas, going from low spin to high spin increases the unit cell volume.

This can be investigated in thin films where the low dimensional geometry creates a localized effect that may enable tuning of the spin crystal defects. Epitaxial strain induced in a thin film due to lattice mismatch with a substrate serves as a versatile controlling parameter of physical and chemical properties, including the electronic structure, conductivity, and crystallographic symmetry. Not only can it fine-tune the properties, but it can also sometimes stabilize novel behaviors, which cannot be found in bulk counterparts. Epitaxial strain is usually associated with a change in in-plane lattice constant accommodated through structural distortions such as changing the internal bond lengths or changing the angle or pattern of rotations and tilts of the oxygen octahedral. For example thin film $LaCoO_3$ (LCO) has been reported to exhibit a long-range ferromagnetic ordering below 80 K, whereas bulk LCO shows a nonmagnetic ground state. In fact, in epitaxial thin films, the mechanical stress due to the lattice mismatch between the film and substrate increases with the film thickness until the critical thickness is reached where the film relaxes.

To understand the microscopic origin of the ferromagnetism and the effect of strain, high quality epitaxial LCO thin films were grown on various substrates to impose different strain states. Woo Seok *et al.* [27] reported that high quality epitaxial thin films exhibited systematic strain dependent distinct dark stripes. For the LCO film grown under slight compressive strain, only a few in-plane stripes were observed. As tensile strain was applied, on the other hand, LCO started to show stripes running perpendicularly to the surface. As the degree of tensile strain increased, more such stripes appeared, eventually forming a fairly regular superstructure. Now, in order to assess the nature of the lattice modulation-induced stripe patterns, interatomic distances from the STEM image were mapped out. The intensity profiles for the red and green lines drawn in Figure 4a and the interatomic spacing between the neighboring La atoms are shown in Figure 4b and c, respectively. While region I (green) showed more or less equal spacing between the La atoms, region II (red) showed a clear spatial modulation, which resulted in vertical dark stripes in the image.

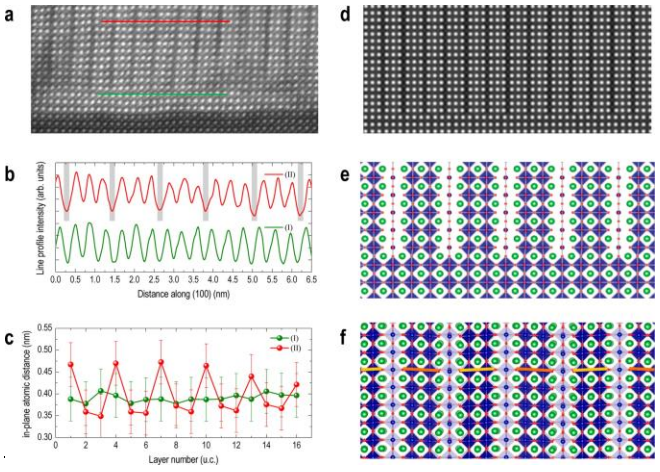

Figure 4: simulation of structural nanodomains. (a) Experimental, cross-sectional STEM image for the LCO film on STO showing the stripes (b) Intensity profile (c) In-plane atomic distances between La atoms (d) Simulated, cross-sectional STEM image for a LCO film (e) Cross-sectional and (f) top views for the artificially constructed LCO film structure. [68]

In the present case, the Co–O bond length in the tetragonally distorted octahedra increased by as much as 0.5 Å due to the local lattice distortion (Figure 4c), which could result in an electronic structure closer to that of a square planar coordination of Co^{3+}. Such an unusual coordination would give rise to a distinctively different orbital occupation and spin state [27].

These studies highlight the collective phenomena in a transition metal oxide, whose magnetic and electronic properties are globally modified by a local structural change. These structural changes can be studied via MBE and UHV to provide an understanding of the relationship between spin state and structure.

3.2.1 Influence of oxygen vacancies on unit cell volume of oxides

In addition to changes in internal bond lengths and octahedral rotations, another possible effect of the change in lattice parameter forced by coherent epitaxy is a change in the defect profile. Such a response is likely because both strain and point defect affects the volume. Aschauer *et al.* [28] used the perovskite $CaMnO_3$ to analyze the strain dependence of the oxygen vacancy formation reaction. When an oxygen vacancy is introduced, high-spin Mn^{3+} (0.645 Å) is most likely to be compensating on Mn^{4+}

(0.53Å) sites, it is clear that the reaction should be accompanied by a considerable volume expansion, which indeed is supported by experiments [29]. Since volume increases (decreases) with tensile (compressive) strain, the oxygen vacancy formation energy is expected to be sensitive to strain. In addition to this volume effect, strain may also affect the oxygen vacancy formation energy through its effect on the electronic energy levels. The electrons from the loss of O_2 which reduce Mn^{4+} to Mn^{3+} occupy the e_g orbitals, the energies of which are strongly affected by the coordination geometry of the surrounding ions. As expected from the known unit cell volume expansion caused by oxygen vacancies, tensile strain was found to lower the formation energy for oxygen vacancies in $CaMnO_3$. Based on the studies cited it is proposed to understand oxygen vacancies and control epitaxial strain, in order to engineer low spin BTO films.

3.3 BTO film growth

BTO thin film is recently being studied extensively due to the fact that the physical properties of BTO in thin films can be tuned or modified due to well-controlled growth conditions, careful selection of substrates, strain effects, interfacial and coupling effects leading to control of crystal structure. This can be explored to further enable the control of the electronic structure, the spin state and hence thermoelectric properties of strong correlated systems like BTO. BTO films have been grown on a variety of substrates by methods such as PLD, sputtering and MBE and those previous experiments have shown that deposition parameters play an important role in tuning the properties of the films. However, there is no literature published with the integration of Iron-doped BTO on SiC MBE. Therefore, a critically analysis of the progress in thin film BTO growth can incorporate the findings and understandings necessary for the successful integration of high quality Fe-BTO thin films on semiconductors with precise control of stoichiometry, crystallinity and orientation necessary for the tuning of its thermoelectric properties.

3.3.1 Influence of growth parameters on BTO film growth

Thin film growth by physical vapor deposition is a nonequilibirium process based on a competition between kinetics and thermodynamic factors. The kinetics (growth rate, adatom migration rate) and thermodynamic equilibrium (growth temperature, phase

stability) parameters strongly influence the thin film crystallinity and crystallographic orientation. The role of the substrate temperature in controlling structure and composition of the film is a primary one. For example, Nb-doped $BaTiO_3$ thin films were deposited $SrTiO_3$ substrates using pulsed laser deposition (PLD) [31]. The substrate temperature was controlled from 575^0C to 800^0C. A higher density of defects in the films grown at 800 °C was found compared to the films grown at 575 °C resulting in a change of lattice symmetry from a tetragonal to a cubic structure with the increase of growth temperature.

$BaTiO_3$ films (~18–20 nm) were grown on $SrTiO_3$/Si under 1×10^{-7} Torr of oxygen at different temperatures ranging from 410 °C to 580 °C [32]. The corresponding RHEED patterns characteristic of the crystallinity, exhibit rings when the temperature exceeds 480 °C. This could denote a polycrystalline surface but all the samples, except the one grown at 580 °C, are found to be single crystalline by X-ray diffraction. Off-stoichiometry might be induced by the temperature, leading to the segregation of Ba on the surface. Moreover, a study by Gonzalo *et al.* showed that Ti/Ba composition of BTO films grown on MgO substrates by pulsed-laser deposition is dependent on the oxygen pressure.

At a given substrate temperature, the literature shows that the O_2 partial pressure also plays an important role on thin film stoichiometry, and structure. For example, Zhao *et al.* observed a dependence of the crystallographic orientation on the oxygen pressure in the range of 1.5×10^{-6} to 10^{-1} Torr for films grown on $SrTiO_3$ by laser MBE [37]. Different deposition processes involving different mechanisms and energy range for the impinging species at the substrate surface show a similar trend with oxygen pressure: an increasing oxygen pressure leads to a change from *c*-axis to *a*-axis growth (although the pressure ranges are necessarily different depending on the techniques). Oxygen pressure is therefore expected to impact the occurrence of oxygen vacancies, the cationic composition, the nature of the defects, and the resulting strain state which is going to impact the spin state of the metal incorporation in BTO.

3.3.2 Doping of BTO

The mechanism of dopant incorporation into barium titanate has been largely investigated [21] [26]. It has been seen that the effect of the specific impurity on BTO crystal structure depends on the substitution site. The ionic radius is one of the main

parameter that determines the substitution site. For example: La^{3+} (1.15 Å) and Nd^{3+} (1.08 Å) are seen to exclusively be incorporated at the Ba (1.35 Å) site, as their size is incompatible with that of Ti^{4+} (0.68 Å) [33]. Other conditions such as dopant concentration and cation ratio can also impact the substitution site as it found by Buscaglia *et al.*[35].

Deka *et al.* investigated the crystal structure, magnetic and dielectric properties of $BaTi_{1-x}Fe_xO_3$ samples for x=0.0–0.3[34]. The un-doped compound was found to crystallize in tetragonal structure while Fe -doped samples are found to crystallize in the mixture of tetragonal and hexagonal phases. Also an increase in lattice parameters and unit cell volume is observed for x= 0.1 and it can be attributed to Fe^{+3} ions (ionic radius, *r*=0.645 Å) replacing the Ti^{+4} (*r*=0.605 Å) ions. The lattice parameters and therefore the structure is predicted to be affect by the dopant concentration and the oxidation state, two factors that have been observed to affect the spin state of a material.

3.3.3 Oxidation state of Fe in BTO

Since all three states of iron ions have the potential to be low spin, it is necessary explore the possibility of Fe^{2+}, Fe^{3+} or Fe^{4+} incorporated in BTO lattice. Theoretical mechanisms based on thermodynamic driving forces and confirmed by experimental data comparison can tell us a lot about what is most like to occur when substituting a metal ion into a metal oxide lattice. Based on Buscaglia *et.al* atomistic simulation study on the incorporation of ions:

A. In BTO, divalent dopants (dopants with valence state 2+) can substitute for either barium or titanium. In the case of Fe^{2+} substitution at the barium site no charge-compensating defect is required because the crystal has a neutral charge, whereas substitution at the titanium site is compensated by an oxygen vacancy to maintain charge neutrality.

B. For, trivalent dopants (dopant with valence state 3+) there are four different incorporation modes. The first and second modes are substitution at the barium site where charge compensation can occur by formation of either conduction electrons or titanium vacancies. The third mode is substitution at the titanium site where the excess negative energy charge is compensated by oxygen vacancies. The fourth mode is self-

compensation which implies simultaneous substitution at the barium and at the titanium site without the creation of electronic or lattice defects for charge compensation.

The number of possible mechanisms for incorporating of a metal in $BaTiO_3$ increases with increasing valence charge of the metal. In the case of Iron (Fe) both Fe^{2+} and Fe^{3+} will substitute at the titanium site. On the other hand, calculations made by Buscaglia *et al.* [35] suggested that direct incorporation of Fe^{3+} is favored in comparison with reduction of Fe^{3+} to Fe^{2+} charge state. Predicting which mechanism is favored is based on simulations calculating the substitution energy of incorporating a dopant in a lattice by systematically adjusting the position of the constituent species (ions) until the minimum energy configuration is found. However, the substitution energies corresponding to different incorporation mechanism were also shown to strongly depend not only on ionic radius but also on growth parameters such as oxygen pressure/environment and Ba/Ti ratio and other factors like the electronic structure, and bonding character of the dopant ions [36].

4.0 EXPERIMENTAL PLAN

It is hypothesized that understanding the spin interaction and the mechanisms of spin state transition in metal oxides can provide insights for successfully engineering thermoelectric materials with Seebeck coefficient values greater than 2000 μV/K, without deteriorating other transport properties. In order to understand the source of Seebeck coefficient enhancement, spin interactions will be observed in a low dimensional geometry that creates a localized effect that may enable the tuning of the spin state of the metal. Iron doped Barium titanate thin film will be used to understand the influences of the processing parameters of the Fe/O ratio, oxygen pressure, substrate temperature and dopant concentration on the oxidation state of the metal and its spin state. In this way we can relate structure and chemistry to processing conditions and to the resulting spin state. In addition, it is important to understand how crystal structure (including defects) and orientation affect the spin state of the oxide film in order to engineer thin films suitable for thermoelectric devices. MBE processing allows the atomic level controlled

environment necessary to study these influences. By utilizing the benefits of UHV and MBE to understand the mechanisms, it will be possible to tune the spin state with precise control of the interfaces between the film and the substrate, the stoichiometry, crystallinity of the film and the film orientation necessary. Three objectives are required to attempt this goal:

Objective 1: Establishing operating condition window for integrating high-quality, smooth single crystal BTO (111) thin films on 6H-SiC (0001)

Objective 2: Understanding growth parameters that will promote the incorporation of low spin iron in BTO films to investigate the oxidation state of Fe as a function of growth parameters and spin state

Objective 3: Correlating growth parameters to spin state.

After meeting these objectives, the influences of such processing parameters as surface structure and chemistry of substrate or interlayer, substrate temperature, and the oxygen pressure on the growth of Fe-BTO should be understood completely. Then, it is expected to successfully incorporate low spin Fe in single crystal BTO on 6H-SiC via MBE and provide new insight into the contribution of spin state in the mechanism of Seebeck coefficient enhancement in metal oxides. If time allows, the testing of the impact of spin state on TE properties will be preliminarily explored.

4.1 Objective 1: Establishing growth conditions for BTO (111)

In objective 1, single crystalline BTO (111) will be integrated on MgO/6H-SiC. 6H-SiC is the substrate of choice due to the fact that SiC maintains semiconductor behavior at much higher temperatures which in turn permits SiC semiconductor device functionality at much higher temperatures which is ideal for high-temperature heat harvesting. Also previous studies in our laboratory have successfully explored the growth of BTO (111) on hexagonal structured substrate 6H-SiC. Success implies the growth of high quality single crystal $BaTiO_3$ thin films with atomically abrupt interfaces. Among those parameters influencing crystal structure and BTO thin film quality, one of the most important is the crystallographic properties of the substrate.

SiC surface preparation is performed using a hydrogen flow furnace on the Si face, this is based on the procedure developed by Dr. Cai Ph.D. study [39]. The SiC

surface after H_2 cleaning should be free of surface contamination and polishing scratches, and terminated by a silicate adlayer [38]. All oxide films in this study will be deposited by molecular beam epitaxy (MBE) in an ultra-high vacuum (UHV) chamber with a base pressure of 1.0×10^{-9} Torr available in the Interface Engineering Laboratory at Northeastern University.

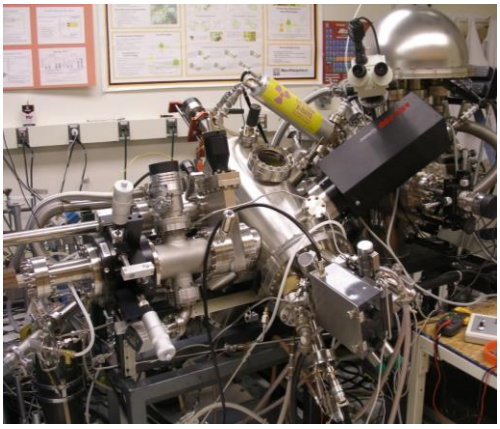

Figure 5: UHV system consisting of two chambers with surface analysis tools

The growth chamber is fitted with a dual source, low temperature effusion cell (for Ba and Mg supply), a high temperature effusion cell (for Fe supply), a Ti-ball sublimator (used for Ti supply) a remote oxygen plasma source, and a RHEED system. The analysis chamber consists of our XPS. The atomic (Ba, Ti, Mg, Fe) fluxes are calculated based on the thermocouple temperature reading and vapor pressure calculations based on equation 6

$$\phi = \frac{3.51\times10^{22} PA}{\pi L^2 \sqrt{MT}} \qquad (6)$$

Where:

ϕ = atomic flux (#/cm^{2}sec)
P = vapor pressure (Torr)
A = aperture area (cm^2)
L = distance from source to substrate (cm)
M = molecular weight (g/mol)
T = temperature (^{o}C)

Based on this equation, increasing the temperature of the appropriate effusion cell, increases the flux of that metal. The opposite is also true. By having the ability to maintain a stable cell temperature to within 1^{o}C, it is possible to tune the individual fluxes to obtain desired film chemistry. Control over the titanium flux is restricted and done by fixing the Ti-Ball power supply which is fixed at 0.5 ^{o}A intervals

The oxygen is supplied through the use of an Oxford Applied Research remote oxygen rf-atom source. The plasma is generated within an Al_2O_3 discharge tube and exited through an Al_2O_3 aperture plate with 276. The size, quantity, and dispersion of the through holes minimized the line-of-site effect associated with UHV and create an oxygen environment at a pressure of 5.0×10^{-6} Torr, which corresponds to an O flux of 3.5×10^{15} atoms/cm^2 sec. Although the oxygen environment is a combination of oxygen species, the flux is represented on the basis of individual atoms and is calculated from the following equation:

$$\phi_O = 2\phi_{O_2} = 2\left(\frac{3.513\times10^{22}P}{\sqrt{MT}}\right) \quad (7)$$

Where:

ϕ = atomic flux (#/cm^{2}sec)
P = chamber pressure (Torr)
M = molecular weight (g/mol)
T = temperature (K)

4.1.1 Growth of template layer for integration of BTO

Perovskite oxide BTO, has a tetragonal crystal structure with a lattice constant of a = 3.992 ^{o}A and the substrate of choice 6H-SiC is arranged in a hexagonal structure with lattice constant of 3.08 A. This creates a very large lattice mismatch of 21% and consequently leads to amorphous BTO film when BTO is deposited directly on hydrogen cleaned 6H-SiC (0001) [38]. When integrated on the MgO (111) template layer, the mismatch between the O-O of BTO (111) and the substrate (O-O of MgO (111)) is reduced to 5.7% compressive, with a 30 degree rotation of the hexagon, and a 5.3 % tensile with no rotation. It was observed that BTO (111) does prefer to tensile mismatch

of 5.3 %. Also it was found that increasing the template layer from 2 nm to 10 nm resulted in formation of some random 3D islands. When increasing the template layer to 40 nm the resulting RHEED pattern was dominated by diffraction from the three-dimensional 3D MgO islands with mixed 60° in-plane rotations. Therefore, a thin (2.5 nm), crystalline MgO (111) template layer will be used for improved epitaxy and crystal structure of tetragonal BTO (111), the expected epitaxial orientation for BTO on a hexagonal substrate.

4.1.2 Growth of BTO on MgO/6H-SiC

One of the key factors contributing to the success of the growth of BTO via MBE is the establishment of a growth window defining the range of growth condition to achieve stoichiometric BTO. The growth of 3 element materials by MBE is complex therefore the first step is to understand the relative fluxes necessary in order to achieve single crystal, stoichiometric BTO (111). For all initial BTO films designed to narrow down the stoichiometry window, growth parameters used in previous work done by Dr. Goodrich Ph.D. study [38] will be used: oxygen species and substrate temperature will be held constant. This will allow the transition from the demonstration of the BTO growth on SiC to understanding mechanisms in order to later grow Iron doped BTO. So, if the co-evaporation of Ba and Ti with a stoichiometric flux is not attained, the stoichiometry will be set by varying the barium flux or the titanium flux. In the case of non-stoichiometry and/or polycrystallinity/amorphous in the BTO (111) film, several other studies will be performed:

1) **Oxygen pressure during growth:** if the films are not stoichiometric oxygen pressure during growth will be varied then
2) a graph of pressure versus stoichiometry (XPS analysis of Ba peaks, O peaks, Ti peaks) will be developed
3) **Substrate temperature study**: In literature it has been seen that substrate temperature causes significant differences in film crystallinity. Each ferroelectric material appears to have a distinct substrate temperature range that is optimum for epitaxial film growth. Therefore, starting with previous work condition of 650 ^{0}C the substrate temperature will be studied to achieve single crystal BTO film
4) **Oxygen Plasma**: control of active oxygen (O_2 vs. O*)

4.2 Objective 2: Understanding the effect growth parameters on Fe-doped BTO

In order to test the feasibility and concept of tuning the spin state of a metal oxide, Fe will be incorporated in BTO via MBE which gives the ability to control mechanism at the atomic level. Using Koshibae *et al.* modified Heikes formula in equation 8, previously introduced in the background:

$$S = \frac{k_B}{q} \ln\left(\frac{g_{(I)}}{g_{(II)}} \frac{y}{1-y} \right). \tag{8}$$

We can hypothesize which oxidation state of Fe ions has the potential to maximize the ratio of degeneracy between oxidation states.

Having a combination of Fe^{2+} and Fe^{3+} enables electron hoping from Fe^{2+} to Fe^{3+} and this exchange might provide spin entropy that can enhance the Seebeck coefficient. The balance between Fe^{2+}/Fe^{3+} needs to be explored. If $BaTi_{1-x}Fe_xO_3$ films are stoichiometric, it is logical to assume that both the Fe and Ti cations have 4+ oxidation states. To compensate for a deficiency of O^{2-} anions in films grown in vacuum, the most likely event is the reduction of Fe^{4+} to Fe^{3+}. Based on literature, in a Ba-Fe-O system, a lot of ternary compounds have been reported, such as $BaFe_2O_4$ ($BaO{\cdot}Fe_2O_3$), $Ba_2Fe_2O_5$ ($2BaO{\cdot}Fe_2O_3$). The first step in doping BTO with Fe is to understand the relative fluxes necessary to incorporate Fe with the proper oxidation states of Fe and Ba and Ti. Controlling the iron oxidation is critical to stoichiometry control, site substitution as well as to the Fe spin state.

In order to have Fe substitute for the Ti, the Fe will be forced to its 3+ oxidation state. Several parameters will be investigated to understand the effect of processing conditions on film stoichiometry, film crystallinity, crystal structure, and chemistry in order to identify potential influences on the spin state of Iron-doped BTO.

1) **Plasma power study**: while O_2 is the most convenient to oxidize metal Ba to Ba^{2+}, is not sufficiently active to allow all metal Fe to form ferric iron (Fe^{3+}) even at O_2 pressures on the order of 10^{-4} Torr. Therefore, the plasma power (watts) will be varied while keeping a constant Ba/Ti ratio and a constant Fe flux to analyze the valence state of metal ion.

- O_2 plasma vs Stoichiometry will be generated (XPS analysis of O peaks, Fe peaks)

2) **O_2 pressure study**: If Fe^{3+} does not substitute in for Ti, oxygen growth pressure will be varied while keeping Ba/Ti ratio constant and Fe flux constant to relate oxygen pressure to the formation of oxygen vacancies and oxidation state of the metal ions. (XPS analysis of Ba, Ti, O and Fe peaks)
   - The ratio of total oxygen to iron Fe flux/O flux will be correlated to the ratio of Fe^{2+}/Fe^{3+}
3) **Temperature study**: If the right chemistry obtains but the film is amorphous then a temperature study will be done to understand its effect on film crystallinity
4) **Dopant concentration study**: Assuming we have single crystal iron substitution. Doping level can be studied: vary Fe flux while keeping Ba/Ti constant, oxygen plasma power constant and oxygen pressure constant analyze the valence state of metal ion and analyzing Fe flux versus stoichiometry (XPS analysis of Ba, Ti, O and Fe peaks)
5) **Fe/Ti ratio study**: Varying Fe/Ti ratio by controlling the Fe and Ti flux independently to analyze the valence state dependence of the metal ions to the substitution of Fe for Ti and to analyze the Fe^{2+}/Fe^{3+} ratio (XPS analysis of Ba, Ti, O and Fe peaks)
6) **Thickness study**: The strain effect on unit cell volume, oxidation state and spin state will be analyzed by changing the thickness and the type of strain.

The Fe and O bonding states can be explore using XPS to understand the role of oxygen vacancies in the thin films. The line shape binding energy positions of Fe2p core level spectra in any compounds depends on the ionic state of Fe, electrostatic interactions, crystal field energy and spin-orbit coupling between the 2p core hole and unpaired 3d electrons of the photoinonized Fe cation. After the growth parameter studies, the effect of those processing parameters (e.g. T_S, P, and fluxes) will be tuned to produce Fe-BTO films on MgO/6H-SiC with the desired chemical structural, metal oxidation state. The spin state corresponding to the desired chemical structure and metal oxidation will be investigated and correlated with thermoelectric properties.

4.3 Objective 3: Correlation of growth parameters to spin state and thermoelectric properties of films.

The spin state of the films will be characterized indirectly from their magnetic properties via Superconducting Quantum Interference Devices (SQUID). The raw data will be processed to obtain molar paramagnetic susceptibility and magnetic moment. Magnetic measurements, particularly for the first row transition elements, give information about the number of unpaired electrons. The number of unpaired electrons provides information about the oxidation state and electron configuration and hence the spin state. Whether the Fe ion is in a low spin or high spin can be found in the magnetic susceptibility and the magnetic moment.

5.0 Summary

In order to investigate the potential TE properties of Fe-BTO via MBE, the influences of processing parameters on the incorporation of low-spin Fe in BTO thin films will be studied to understand the atomic level relationship between spin state and Seebeck coefficient of metal oxides which can result in high tunable TE properties. To complete the proposed goal and objectives detailed studies represented will be performed and proposed timeline is included in Figure 6.

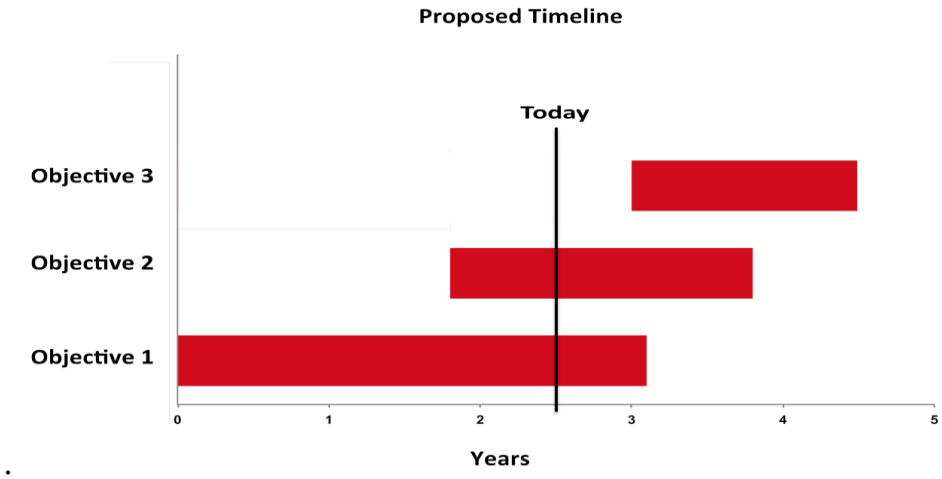

.

Figure 6: Proposed timeline for completing objectives and aims

6.0 References

1. X. Zhang and L.D. Zhao. Journal of MateriomicsVolume 1, Issue 2, June 2015, Pages 92–105
2. L.D. Zhao, S.H. Lo, Y.Zhang, H. Sun, G. Tan, C. Uher, C. Wolverton, V.P. Dravid and M. G. Kanatzidis. *Nature* **508**,373–377
3. Rowe, D.M, *CRC Hanbook of thermoelectrics*
4. The Donald Morelli Research Group. Michigan state university http://www.egr.msu.edu/morelli-research/thermoelectrics.html
5. Z. Dughaish, "*Lead Telluride as a Thermoelectric Material for Thermoelectric Power Generation*," Physica B*, vol. 322*, pp. 205-223, 2002.
6. D.Vasileska, and S. Goodnick, *Nano-Electronic Devices: Semiclassical and Quantum Transport Modeling*. 2011
7. G. J. Snyder, E. S. Toberer, *Nat. Mater.* 7, 105 (2008), 105 - 114
8. W.E pickett, "*Electronic Structure of the High-temperature Oxide Superconductors*," Rev. Mod. Phys. **61**, 433, 1989.
9. G.Michael USGS Minerals Information: Selenium and Tellurium. USGS 2010 Minerals Yearbook (2010).
10. Wang Y., Nyrissa S. Rogado, R. J. Cava & N. P. Ong, "*Spin entropy as the likely source of enhanced thermopower in* $Na_xCo_2O_4$". Nature 423, 425-428 (22 May 2003)
11. Rodgers G.E. "Descriptive Inorganic, Coordination, and Solid-State Chemistry" 3rd Edition, 2012.
12. Gao G., Reibstein S., Spiecker E., Peng M. and Wondeaczek L., "*Broadband NIR photoluminescence from Ni2+- doped nanocrystalline Ba-Al titanate glass ceramics*" J. Mater. Chem., **22**, 2582-2588, 2012
13. J. H. Haeni, P. Irvin, W. Chang, R. Uecker, P. Reiche, Y. L. Li, S. Choudhury, W. Tian, M. E. Hawley, B. Craigo, A. K. Tagantsev, X. Q. Pan, S. K. Streiffer, L. Q. Chen, S. W. Kirchoefer, J. Levy, and D. G. Schlom, "*Room-temperature ferroelectricity in strained* $SrTiO_3$," Nature, vol. 430, pp. 758-761, 2004.
14. Cai Z., Chen Z., Goodrich T. L., Harris V. G., and Ziemer K. S., "*Chemical and structural characterization of barium hexaferrite films deposited on 6H-SiC with and without MgO/BaM interwoven layers*," Journal of Crystal Growth, vol. 307, p. 321, 2007.
15. Kennedy, R.J. and a.P.A. Stampe, *Fe3O4 films grown by laser ablation on Si(100) and GaAs(100) substrates with and without MgO buffer layers.* J. Phys. D: Appl. Phys., 1999 **32**: p. 16-21.Growth mechanism and structure of epitaxial perovskite thin film and superlattices (Dissertation 2003)
16. Ray, R.; Ghoshray, A.; Ghoshray, K.; Nakamura, S. Co NMR studies of metallic $NaCo_2O_4$. *Phys. Rev. B* 1999, *59*, 9454–9461.
17. Terasaki, I., Sasago, Y. & Uchinokura, K. *Large thermoelectric power in NaCo2O4 single crystals*. Phys. Rev. B 56, R12685–R12687 (1997).
18. Kobayashi W. *et al. "Room-temperature ferromagnetism in* $Sr_{1-x}Y_xCoO_{3-\delta}$ *(0.2 ≤ x ≤ 0.25)*. Phys. Rev. B 2005, 72, 104408.

19. Kobayashi, Y., Mogi, T., Asai, K., *Spin-state transition in $La_{1-x}Pr_xCoO_3$*. J. Phys. Soc. Jpn. 2006, 75, 104703.
20. Baier, J., Jodlauk, S., Kriener, M., Reichl, A., Zobel, C., Kierspel, H., Freimuth, A., Lorenz, T. "*Spin-state transition and metal-insulator transition in $La_{1-x}\,Eu_x\,CoO_3$*" Phys. Rev. B 2005, 71.
21. Tang G. D. *et al.*, "*The spin entropy suppression induced by Fe^{3+} in $NaCo_2O_4$,* J. Appl. Phys. **107**, (2010)
22. Park K., and Jang K. U., *Mater. Lett.* **60**, 1106 (2006)
23. Terasaki I. *et al. Phys. Rev. B* **65**, 195106 (2002)
24. Kozhevnikov, A.V., Lukoyanov, A.V., Anisimov, V.I., and Korotin, M.A. "*Transition of Iron Ions from High-Spin to Low-spin state and pressure-Induced Insulator-Metal Transition in Hematite Fe_2O_3*". Electronic Properties Of Solids. (2007) 105:1035.
25. Linares J., Codjovi E., and Garcia Y., *Pressure and Temperature Spin Crossover Sensors with Optical Detection.* Sensors 2012, 12, 4479-4492
26. Gütlich, P., Goodwin, H.A., "Spin Crossover in Transition Metal Compounds II", 2004
27. Choi W.S.,KwonJ.H., Jeen H., Hamann-Borrero J.E, Radi A., Macke S., Sutarto R., He F., Sawatzky G.A., Hinkov V., Kim M. and Nyung Lee H. Nano Letters 2012 12 (9), 4966-4970
28. Aschauer U., Pfenninger R., Selbach S. M, Grande T., and Spaldin N. A., "*Strain controlled oxygen vacancy formation and ordering in $CaMnO_3$*" Phys. Rev. B, **88**, 054111, 2013.
29. Chen X., Yu J., and Adler S. B., Chem. Mater. 17, 4537 (2005)
30. S. Inoue *et al.* "*Anisotropic oxygen diffusion at low temperature in perovskite-structure iron oxides"*. Nature Chem. 2, 213–217 (2010).
31. Kim Y.H., Lu X., Diegel M., Roland M., Hesse D., Alexe M., "*Growth temperature dependence of crystal symmetry in Nb-doped BaTiO3 thin film*," Journal of Advanced Dielectrics, vol. 3, No.2 (2013)
32. Mazet L., Bachelet R., Louahadj L., Albertini D., Gautier B., Cours R., Schamm-Chardon S., Saint- Girons G., Duboudieu C., "*Structural study and ferroelectricity of epitaxial BaTiO3 films on silicon grown by molecular beam epitaxy*" J. Appl. Phys. 116, 214102 (2014)
33. Gilman, P.S.,Benjamin, J.S., *Mechanical Alloying*, *Ann. Rev. Mater.Sci.*, 198 3 (13) 279-300.
34. Deka B., Ravi S., Alagarsamy P., Pamu D., " *Ferromagnetism and ferroelectricity in Fe-doped BaTiO3*" Physica B Condensed Matter, 448: 204-206 (2014)
35. Buscaglia, M.T., Buscaglia V., Viviani, M., J. Am. Ceram. Soc. 84[2] 376-84 (2001)
36. Zhi, J., Chen, A., Zhi, Y., Vilarinho, P. Baptista, J.L., *J. Am. Ceram. Soc.*, 82(5) 1345–48 (1999)
37. Zhao T., Chen F., Lu H., Yang G., and Chen Z. "*Thickness and oxygen pressure dependent structural characteristics of $BaTiO_3$ thin films grown by laser molecular beam epitaxy"*. J. Appl. Phys. **87**, 7442 (2000)

38. Goodrich, T.L., "*Atomistic Investigation into the Interface Engineering and Heteroepitaxy of Functional Oxides on Hexagonal Silicon Carbide through the Use of a Magnesium Oxide Template Layer for the Development of a Multifunctional Heterostructure*". (2008)
39. Cai, Z., "*Molecular beam epitaxy integration of magnetic ferrites with wide bandgap semiconductor 6H-SiC for next-generation microwave and spintronic devices*", 2010, Ph.D. Dissertation, Boston, MA, Northeastern University.